Superhorizon fluctuations and the cosmic dipole problem*

Ge Chen (陈戈)[1] Chengcheng Han (韩成成)[1,2†] Linwei Qiu (邱林蔚)[1]

[1]School of Physics, Sun Yat-Sen University, Guangzhou 510275, P. R. China
[2]Asia Pacific Center for Theoretical Physics, Pohang 37673, Korea

Abstract: Recent observations have identified a significant 4.9σ tension between the cosmic dipole inferred from galaxy number counts and that derived from the Cosmic Microwave Background (CMB), suggesting a potential deviation from the cosmological principle. This work investigates whether superhorizon isocurvature perturbations in cold dark matter (CDM) can account for this discrepancy. We demonstrate that, unlike adiabatic modes, which cancel at leading order, superhorizon isocurvature modes can generate an intrinsic CMB dipole without significantly affecting galaxy number counts, thereby explaining the observed mismatch. We explore both single-mode and continuous-spectrum cases, focusing on two concrete models: a nearly scale-invariant power-law spectrum with a UV cutoff and axion-induced isocurvature perturbations. For the axion scenario, we show that if the radial mode evolves during inflation, the resulting perturbations can match the required amplitude while evading current CMB constraints. Our analysis constrains the self-coupling of the axion potential to the range $10^{-9} < \lambda < 4\times10^{-9}$. These findings offer a viable solution to the dipole tension and may serve as indirect evidence for axion dark matter.

Keywords: CMB, Cosmological perturbation, Axion

DOI: 10.1088/1674-1137/ae6b2e **CSTR:**

I. INTRODUCTION

The cosmological principle asserts that the universe is homogeneous and isotropic on large scales; it is a fundamental assumption underpinning many key results in modern cosmology. Ellis and Baldwin [1] note that the cosmic rest frame (CRF) of galaxies and dark matter should coincide with that of the Cosmic Microwave Background (CMB) if the cosmological principle holds, providing a powerful consistency test of the Friedmann-Lemaître-Robertson-Walker (FLRW) models. If the observed CMB dipole anisotropy is indeed kinematic due to our local peculiar motion with respect to the CRF, then there must be a corresponding kinematic dipole imprinted in the galaxy number counts across the sky [1−5].

However, recent studies have found a significant discrepancy between the cosmic dipole inferred from galaxy number counts and that derived from the CMB, suggesting that the two CRFs do not align [5−14]. Notably, distant radio galaxies and quasars exhibit a dipole amplitude 2–3 times larger than predicted by the kinematic interpretation of the CMB dipole, with the highest reported tension currently approximately 4.9σ [13−18]. The apparently large dipole in galaxy number counts raises doubts about the validity of the cosmological principle or suggests that systematic effects may have been underestimated [19−21].

It is conceivable that matter may exhibit a relative velocity with respect to the CMB if a significant superhorizon cold dark matter (CDM) isocurvature perturbation exists [22, 23]. Turner [24] proposed that such a primordial isocurvature mode with a wavelength much larger than the Hubble radius does not appear as a fluctuation, but rather as a linear gradient across our observable universe. This gradient provides a mechanism for decoupling the CMB rest frame from the matter rest frame. Turner referred to this possibility as a "tilted universe," in which galaxies appear to undergo a bulk motion relative to the CMB rest frame. Subsequent studies have explored the effects of superhorizon fluctuations on the CMB in detail [23, 25], establishing that only isocurvature modes can generate a leading-order CMB dipole. Furthermore, there are other theoretical frameworks that may reconcile this tension, including local bulk flows [26−28], anisotropic inflationary models [29−31], and the dipole ΛCDM model [32], among others. In this work, we focus on the "tilted universe" scenario.

To address the cosmic dipole problem by invoking a significant superhorizon isocurvature perturbation, a concrete model capable of generating such modes is required.

Received 8 August 2025; Accepted 7 May 2026

* This work is supported by the National Key R&D Program of China under grant 2023YFA1606100 and by the National Natural Science Foundation of China under grant No. 12435005

† E-mail: hanchch@mail.sysu.edu.cn

In [23], a single mode of isocurvature perturbation was studied as a possible resolution of the cosmic dipole problem. In this paper, we instead consider a continuum spectrum. In particular, we study two models: one in which the isocurvature power spectrum follows a nearly scale-invariant power law,

$$\mathcal{P}_S(k) = A_I(k/k_{\max})^{n-1}\theta(k_{\max}-k)\,, \tag{1}$$

where θ is the Heaviside step function. To remain consistent with CMB isocurvature bounds, in the first model we require the power spectrum to have a UV cutoff at a sufficiently high wavenumber, $k_{\max}$. In the second model, the isocurvature perturbation is generated by axion dark matter as proposed in [33]. Axions are hypothetical particles arising from the spontaneous breaking of the Peccei-Quinn (PQ) symmetry, a mechanism originally introduced to resolve the strong CP problem in quantum chromodynamics (QCD) [34, 35]. If the PQ symmetry is spontaneously broken during inflation, axion dark matter can generate isocurvature perturbations whose amplitude is set by the Hubble scale, $H/(\pi f_a\theta_0)$ [33, 36–47]. These perturbations are distinct from and uncorrelated with primordial curvature perturbations. Because no isocurvature mode has been detected in current CMB data, stringent constraints are placed on both the axion dark matter fraction and the amplitude of axion isocurvature perturbations [48]. Consequently, if axion dark matter generates large isocurvature perturbations on superhorizon scales during inflation, then they must decay to sufficiently small levels by the recombination scale, $k_{\rm dec}$ [33].

In this paper, we provide a brief overview of galaxy number counts, CMB temperature fluctuations, and the cosmic dipole tension in Section 2. In Section 3, we examine these fluctuations in the presence of a single superhorizon mode, considering both adiabatic and CDM isocurvature modes. In Section 4, we extend the analysis to a continuous spectrum of fluctuations for a more realistic scenario, where we evaluate two models: a power-law spectrum and one based on the axion isocurvature model.

II. THE COSMIC DIPOLE PROBLEM: A REVIEW

Owing to our peculiar velocity, a dipole anisotropy is observed in the Cosmic Microwave Background (CMB). This CMB dipole has been measured to be [49]

$$D_1^{\rm CMB} = (1.23357 \pm 0.00036)\times 10^{-3}\,, \tag{2}$$

from which our peculiar velocity is inferred to be

$$|v_\odot^i| = 369.82 \pm 0.11\ \text{km/s}\,. \tag{3}$$

This velocity also induces a dipole in the galaxy number counts, as discussed in [1]

$$D^{\rm N}_{\rm kin}(\mathbf{n}) = [2 + x(1+\alpha)]v_\odot^i n_i/c\,, \tag{4}$$

where the parameter x characterizes the slope of the cumulative number of sources above a flux threshold, following the relation $N(>S)\propto S^{-x}$, and α is the spectral index of the galaxy sources, assuming a power-law luminosity spectrum $L(\nu)\propto\nu^{-\alpha}$. For the CatWISE quasar catalogue [13, 14], the measured average values are $\langle x\rangle \simeq 1.7$ and $\langle\alpha\rangle \simeq 1.26$. Based on these parameters, if both the CMB dipole and the galaxy number-count dipole are entirely due to our peculiar velocity $v_\odot$, the galaxy dipole amplitude is expected to be roughly four times the CMB dipole amplitude. However, the observed galaxy dipole is about twice as large as this prediction, as reported in [13, 50]:

$$D^{\rm N}_{\rm kin}(\mathbf{n}) = (15.5 \pm 1.7)\times 10^{-3}\,. \tag{5}$$

It points in a similar direction. This suggests a peculiar velocity of

$$v_\odot^i = 797 \pm 87\ \text{km/s}\,. \tag{6}$$

This value deviates by approximately 5σ from the velocity inferred from the CMB dipole measurement.

To account for this discrepancy, we consider the possibility that it arises from superhorizon perturbations. Working in the conformal Newtonian gauge, we adopt the perturbed Friedmann–Robertson–Walker (FRW) metric:

$$ds^2 = a^2(\tau)\left[-(1+2\Psi)d\tau^2 + (1-2\Phi)\delta_{ij}dx^i dx^j\right]\,. \tag{7}$$

In both the CMB and galaxy number-count fluctuations, the total density fluctuation can be decomposed into two components: a kinematic part, arising from the observer's peculiar motion, and an intrinsic part, generated by the perturbations themselves. Accordingly, the fluctuation can be expressed as

$$\Delta(\mathbf{n}, z) = D_{\rm kin}(\mathbf{n}) + \Delta_{\rm in}(\mathbf{n}, z)\,. \tag{8}$$

Observer motion also contributes to the quadrupole at $O(v^2)\sim 10^{-6}$. This kinematic quadrupole is subdominant relative to the intrinsic primordial quadrupole ($\sim 10^{-5}$) and to the $O(v)$ dipole tension that we aim to address. Thus, restricting the analysis to linear order in the velo-

city v and neglecting higher-order terms is sufficient. The CMB temperature fluctuation is then given by [25, 51]:

$$\Delta_{\rm in}^{\rm CMB}(\mathbf{n}) = \frac{1}{4}\delta_r + \Psi + \int_0^{r_{\rm dec}} dr\,(\Phi' + \Psi') + v_o^i n_i - v_s^i n_i\,, \tag{9}$$

$$D_{\rm kin}^{\rm CMB}(\mathbf{n}) = v_\odot^i n_i / c\,, \tag{10}$$

where δ_r is the radiation density contrast, v_s is the velocity potential at the source, $v_i = \partial_i v$, and $v_o = v(\tau = 0)$. The terms $\frac{1}{4}\delta_r + \Psi$, $\int_0^{r_{\rm dec}} dr\,(\Phi' + \Psi')$, and $v_o^i n_i - v_s^i n_i$ correspond to the Sachs–Wolfe effect, the integrated Sachs–Wolfe effect, and the Doppler effect, respectively. The term $v_\odot^i n_i$ denotes the observer's contribution.

The galaxy number-count fluctuation is given by [1, 52, 53]:

$$\begin{aligned}\Delta_{\rm in}^{\rm N}(\mathbf{n},z) = &\left(2 + \frac{\mathcal{H}'}{\mathcal{H}^2} + \frac{2-5s}{r_s\mathcal{H}} - f_{\rm evo}\right) v_o^i n_i \\ &+ b\delta_{mc} + (3 - f_{\rm evo})\mathcal{H} v_s + \Psi \\ &- (2-5s)\Phi + \frac{1}{\mathcal{H}}[\Phi' + \partial_r(v_s^i n_i)] \\ &+ \left(\frac{\mathcal{H}'}{\mathcal{H}^2} + \frac{2-5s}{r_s\mathcal{H}} + 5s - f_{\rm evo}\right) \\ &\times \left(\Psi + v_s^i n_i + \int_0^{r_s} (\Psi' + \Phi')dr\right) \\ &+ \frac{2-5s}{2r_s}\int_0^{r_s}\left(2 - \frac{r_s - r}{r}\nabla_\Omega^2\right)(\Psi + \Phi)dr\,,\end{aligned} \tag{11}$$

$$D_{\rm kin}^{\rm N}(\mathbf{n}) = [2 + x(1+\alpha)] v_\odot^i n_i / c\,, \tag{12}$$

where δ_{mc} is the comoving matter density contrast. b, $f_{\rm evo}$, and s denote the galaxy bias, magnification bias, and evolution bias, respectively; these depend on the specifics of the galaxy survey and instrument. Following [23], we rewrite Eq.(11) in terms of three separate contributions:

$$\Delta_{\rm in}^{\rm N}(\mathbf{n},z) = \Delta_{\rm in}^{(\rm n)}(\mathbf{n},z) + f_{\rm evo}\Delta_{\rm in}^{(\rm evo)}(\mathbf{n},z) + (2-5s)\Delta_{\rm in}^{(\rm s)}(\mathbf{n},z)\,, \tag{13}$$

which allows us to compute each term independently of the biases b, s, and $f_{\rm evo}$.

Reconciling the CMB and galaxy number-count dipoles

Within our observable patch, a superhorizon perturbation can be approximated as a slowly varying gradient. It therefore does not manifest as an ordinary subhorizon inhomogeneity, but rather as a large-scale background modulation across the observable Universe. The crucial point is that adiabatic and isocurvature long-wavelength modes affect the dipole in different ways. For an adiabatic mode, the leading contribution to the dipole cancels among the observer, source, and gravitational terms. This cancellation reflects the fact that a purely adiabatic superhorizon mode can be locally absorbed into a coordinate redefinition at leading order. By contrast, a CDM isocurvature perturbation represents a relative fluctuation between matter and radiation. This relative mode cannot be removed by the same argument and thus can generate an intrinsic CMB dipole [23, 25, 54].

The essential observation is that this intrinsic contribution primarily affects the CMB dipole, while its impact on the late-time galaxy number-count dipole is suppressed. Consequently, the galaxy number-count dipole can still be interpreted, to a good approximation, as tracing the observer's true peculiar motion, whereas the observed CMB dipole receives both kinematic and intrinsic contributions. If the intrinsic CMB dipole is approximately anti-aligned with the kinematic CMB dipole, the observed CMB dipole is smaller than the value inferred from galaxy number counts. This offers a possible way to reconcile the CMB dipole with the galaxy number-count dipole.

Let D_1 denote the dipole amplitude. Since the observed CMB dipole and the galaxy number-count dipole are nearly aligned, we focus on this configuration and write the observed CMB dipole amplitude schematically as

$$D_1^{\rm CMB} = D_{1,\rm kin}^{\rm CMB} - D_{1,\rm in}^{\rm CMB}\,. \tag{14}$$

Here $D_{1,\rm kin}^{\rm CMB} = v_\odot/c$ denotes the kinematic contribution inferred from the galaxy number-count dipole, whereas $D_{1,\rm in}^{\rm CMB}$ denotes the intrinsic contribution sourced by a superhorizon CDM isocurvature mode. The minus sign indicates that the intrinsic dipole is assumed to be opposite in sign to the kinematic CMB dipole. This cancellation is required because the velocity inferred from the observed CMB dipole is smaller than that inferred from galaxy number counts.

Using the galaxy-inferred velocity

$$v_\odot = 797 \pm 87\ {\rm km/s}\,, \tag{15}$$

and the observed CMB dipole amplitude,

$$D_1^{\rm CMB} = 1.23 \times 10^{-3}\,, \tag{16}$$

we find that the required intrinsic CMB dipole is

$$D_{1,\mathrm{in}}^{\mathrm{CMB}} = \frac{v_\odot}{c} - 1.23\times10^{-3} \simeq 1.4\times10^{-3} + \frac{v_\odot - 797\ \mathrm{km/s}}{c}\,. \quad (17)$$

Considering the uncertainty in $v_\odot$, the required intrinsic dipole falls within the 2σ range

$$8\times10^{-4} \lesssim D_{1,\mathrm{in}}^{\mathrm{CMB}} \lesssim 2\times10^{-3}\,. \quad (18)$$

For later use, we recast this requirement as a constraint on the angular power spectrum. We define:

$$C_\ell \equiv \frac{1}{2\ell+1}\sum_{m=-\ell}^{\ell}|a_{\ell m}|^2\,. \quad (19)$$

For a pure dipole modulation, where $\Delta T/T = D_1\cos\theta$, one has

$$D_1 = \sqrt{\frac{9C_1}{4\pi}}\,. \quad (20)$$

Therefore, the intrinsic CMB dipole generated by a superhorizon isocurvature perturbation should satisfy

$$9\times10^{-7} \lesssim C_{\mathrm{in},1}^{\mathrm{CMB}} \lesssim 5.6\times10^{-6}\,. \quad (21)$$

This range corresponds to an intrinsic CMB dipole that is large enough to partially cancel the kinematic CMB dipole, while remaining consistent with the observed large-scale CMB anisotropies. In realistic cosmological models, perturbations are not expected to be dominated by a single Fourier mode but rather by a continuous spectrum. In the following sections, we therefore analyze both a single superhorizon mode and continuous spectra of CDM isocurvature perturbations.

III. THE EFFECT OF A SINGLE PLANE WAVE

For a single superhorizon mode with wavenumber k, the metric perturbation can be written as $\Psi(x,\tau) = \Psi_k(\tau)e^{i\mathbf{k}\cdot\mathbf{r}}$. Using Rayleigh's plane-wave expansion:

$$e^{ik\cdot r} = \sum_{l=0}^{\infty}\sum_{m=-l}^{l} a_{lm}Y_{lm}(\hat{\mathbf{r}}) = 4\pi\sum_{l=0}^{\infty}\sum_{m=-l}^{l} i^l j_l(kr)Y_{lm}^*(\hat{\mathbf{k}})Y_{lm}(\hat{\mathbf{r}})\,, \quad (22)$$

where $j_l(x)$ is the spherical Bessel function and $Y_{lm}(\hat{\mathbf{r}})$ is a spherical harmonic. We then have

$$a_{lm}^{\mathcal{I}} = 4\pi i^l X^{\mathcal{I}}\mathcal{T}_l^{\mathcal{I}}(k)Y_{lm}^*(\hat{\mathbf{k}})\,,$$
$$a_{lm} = 4\pi i^l\left(\sum_{\mathcal{I}} X^{\mathcal{I}}\mathcal{T}_l^{\mathcal{I}}(k)\right)Y_{lm}^*(\hat{\mathbf{k}})\,, \quad (23)$$

where $\mathcal{I}$ labels perturbation modes corresponding to different initial conditions, and $\mathcal{T}^{\mathcal{I}}$ is the corresponding transfer function for X such that $X(\tau,k) = \mathcal{T}(\tau,k)X_{\mathrm{ini}}$.

Since we have assumed that the intrinsic dipole is aligned with the kinematic dipole, we choose the z-direction to be aligned with the CMB kinematic dipole and expand the plane-wave fluctuation in powers of $(kr_{\mathrm{dec}}\cos\theta)$ and in spherical harmonics. For $\hat{\mathbf{k}} = \hat{\mathbf{z}}$, all Y_{lm} with $m \neq 0$ then vanish and thus

$$\Delta(\hat{\mathbf{r}},z) = \sum_l \frac{1}{l!}D_l(kr_{\mathrm{dec}}\cos\theta)^l = \sum_l a_{l0}Y_{l0}(\theta,\varphi)\,. \quad (24)$$

By comparing the coefficients of each $\cos^l\theta$ term, we can express D_l in terms of the a_{l0} coefficients for a plane wave propagating along the z-direction.

A. CMB fluctuations

We define $\mathcal{T}_X^{\mathcal{I}}(\tau,k)$ as the transfer function of the variable X at conformal time τ and comoving wavenumber k.

$$X^{\mathrm{ad}}(\tau,k) = \mathcal{T}_X^{\mathrm{ad}}(\tau,k)\Phi_{\mathrm{ini}} \quad \text{or} \quad X^{\mathrm{iso}}(\tau,k) = \mathcal{T}_X^{\mathrm{iso}}(\tau,k)S_{\mathrm{ini}}\,. \quad (25)$$

This relation holds for either adiabatic or isocurvature perturbations. Substituting these transfer functions into Eqs. (9) and (10) and projecting onto spherical harmonics, we find that the coefficients a_{lm} are given by

$$a_{lm} = 4\pi i^l\left[F_l^{\mathrm{ad}}(k)\Phi_{\mathrm{dec}} + F_l^{\mathrm{iso}}(k)S_{\mathrm{dec}}\right]Y_{lm}^*(\hat{\mathbf{k}})\,, \quad (26)$$

where

$$F_l^{\mathcal{I}}(k) = \left(\frac{1}{4}\mathcal{T}_{\delta_r}^{\mathcal{I}} + \mathcal{T}_\Psi^{\mathcal{I}}\right)j_l(kr) + \int_0^{r_{\mathrm{dec}}} dr\,(\mathcal{T}_\Phi^{\mathcal{I}} + \mathcal{T}_\Psi^{\mathcal{I}})'\,j_l(kr)$$
$$+ \mathcal{T}_v^{\mathcal{I}}\,j_l'(kr) - \mathcal{T}_v^{\mathcal{I}}(0)j_l'(0)\,. \quad (27)$$

Here, the first two terms arise from the Sachs-Wolfe and integrated Sachs-Wolfe effects, while the last two stem from the Doppler contribution evaluated at the source and at the observer. For simplicity, we consider a combination of a superhorizon adiabatic mode and a CDM isocurvature mode. Neglecting higher-order terms and evaluating the system at decoupling, we use the `CLASS` and `CLASSgal` codes [55, 56] to numerically compute the first

three multipole moments as

$$D_1 = -(kr_{\rm dec})\cdot 0.27 S_{\rm dec}\,, \tag{28}$$

$$D_2 = -(kr_{\rm dec})^2\cdot(0.33 S_{\rm dec} + 0.32\Phi_{\rm dec})\,, \tag{29}$$

$$D_3 = -(kr_{\rm dec})^3\cdot(0.33 S_{\rm dec} + 0.34\Phi_{\rm dec})\,. \tag{30}$$

These correspond to the dipole, quadrupole, and octopole moments, respectively.

As shown in the bottom-right panel of Fig. 1, the leading-order intrinsic CMB dipole generated by adiabatic perturbations is canceled by the kinematic contribution, leaving only the initial isocurvature component to affect the CMB dipole. The coefficients associated with the adiabatic mode are consistent with those reported in [23, 25]. However, the coefficients for the isocurvature mode are approximately 1.5 times as large as those reported in [23].

B. Galaxy number-count fluctuations

We now proceed to study the effect of a monochromatic superhorizon mode on galaxy number-count fluctuations. Because the isocurvature perturbation has not been fully converted into curvature perturbations by the present epoch, a residual CDM isocurvature density fluctuation remains. However, at redshift $z\sim 1$ the associated density contrast is suppressed by a factor of $a_0/a_{\rm eq}\sim 10^3$. Hence, the initial isocurvature perturbation can be safely neglected when assessing its impact on galaxy number counts [23]. We therefore focus only on the adiabatic mode for galaxy number-count fluctuations and write the spherical-harmonic coefficient a_{lm} as

$$a_{lm}(\tau_S) = 4\pi i^l F_l^{\rm ad}(\tau_S,k)\Phi_{\rm ini}Y^*_{lm}(\hat{\mathbf{k}})\,, \tag{31}$$

where [52]

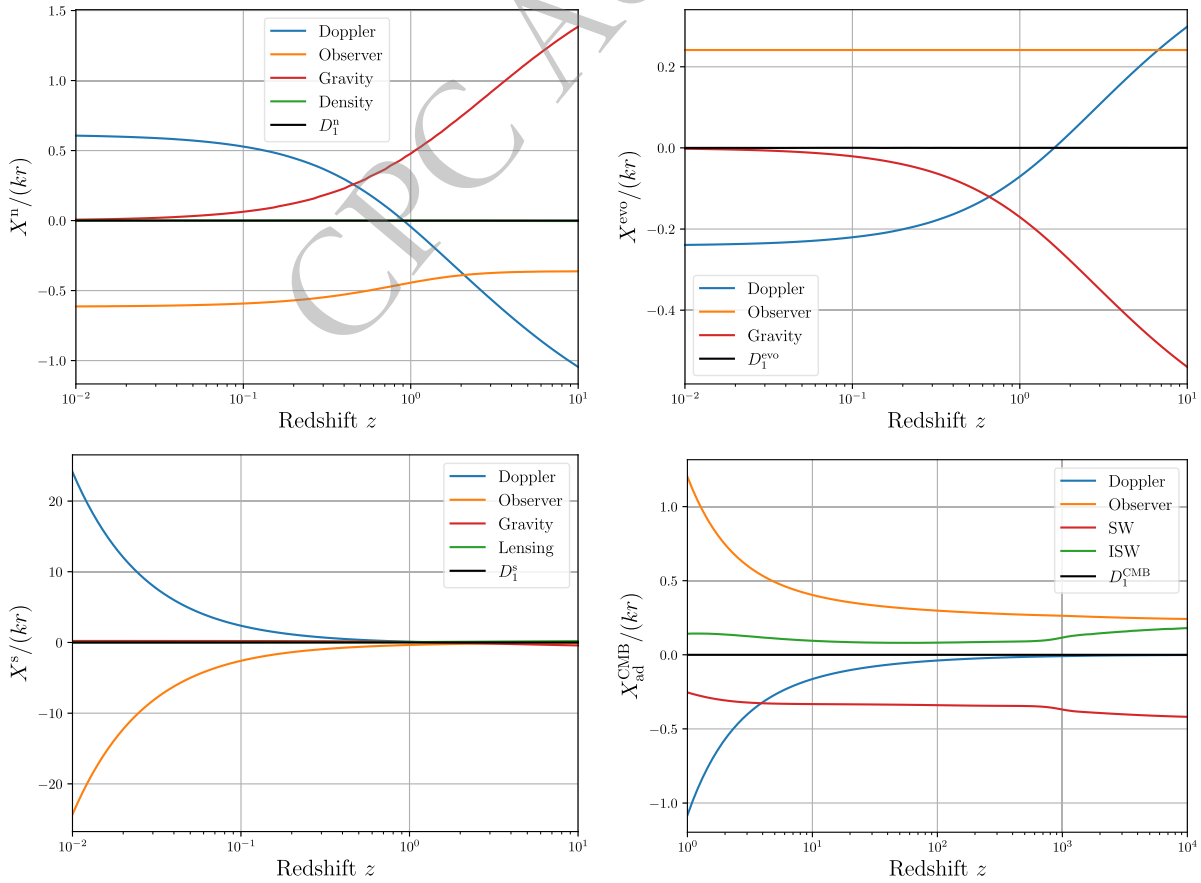

Fig. 1. (color online) Contributions to the number-count dipole and the CMB dipole for a single Fourier mode under adiabatic initial conditions. The first three panels show the contributions to D_1^n [top-left], $D_1^{\rm evo}$ [top-right], and D_1^s [bottom-left], as defined in Eq. (13). The last panel shows the contributions to $D_1^{\rm CMB}$ [bottom-right] from the Sachs-Wolfe effect, the Doppler effect, the integrated Sachs-Wolfe effect, and the observer term. Notably, an exact cancellation occurs, yielding $D_1=0$ (black) to leading order in both the CMB and number-count dipoles for adiabatic initial conditions.

$$
\begin{aligned}
F_l(\tau_S,k) = {} & j_l(kr_S)\left[b\mathcal{T}_\delta + \left(\frac{\mathcal{H}'}{\mathcal{H}^2} + \frac{2-5s}{r_S\mathcal{H}} + 5s - f_{\rm evo} + 1\right)\mathcal{T}_\Psi + (-2+5s)\mathcal{T}_\Phi + \mathcal{H}^{-1}\mathcal{T}_\Phi'\right] \\
& + \left[j_l'(kr_S)\left(\frac{\mathcal{H}'}{\mathcal{H}^2} + \frac{2-5s}{r_S\mathcal{H}} + 5s - f_{\rm evo}\right) + j_l''(kr_S)\frac{k}{\mathcal{H}} + (f_{\rm evo}-3)j_l(kr_S)\frac{\mathcal{H}}{k}\right]\mathcal{T}_V \\
& + \frac{2-5s}{2r_S}\int_0^{r_S} dr\; j_l(kr_S)(\mathcal{T}_\Phi + \mathcal{T}_\Psi)\left[l(l+1)\frac{r_S - r}{r} + 2\right] + \int_0^{r_S} dr\; j_l(kr_S)(\mathcal{T}_\Phi' + \mathcal{T}_\Psi')\left(\frac{\mathcal{H}'}{\mathcal{H}^2} + \frac{2-5s}{r_S\mathcal{H}} + 5s - f_{\rm evo}\right) \\
& - j_l'(0)\left(2 + \frac{\mathcal{H}'}{\mathcal{H}^2} + \frac{2-5s}{r_S\mathcal{H}} - f_{\rm evo}\right)\mathcal{T}_V(0)\,. \qquad (32)
\end{aligned}
$$

We rewrite Eq. (32) in terms of three distinct contributions:

$$
F_l(\tau_S,k) = F_l^{(n)} + f_{\rm evo}F_l^{(\rm evo)} + (2-5s)F_l^{(s)}\,. \qquad (33)
$$

This decomposition allows us to compute each term independently of the biases b, s, and $f_{\rm evo}$. Under adiabatic initial conditions, as shown in Fig. 1, the leading-order contributions cancel in both the galaxy number-count dipole and the CMB dipole. The relativistic contributions — including the Doppler, observer, gravitational, and density terms — are computed numerically with the `CLASS` and `CLASSgal` codes [55, 56].

Thus, to account for the dipole anomaly, we can infer our peculiar velocity from the galaxy number-count dipole as

$$
v_\odot^i = 797 \pm 87\ {\rm km/s}\,, \qquad (34)
$$

which, in turn, induces a kinematic CMB dipole of

$$
D_{1,\rm kin}^{\rm CMB} = (2.7 \pm 0.29)\times 10^{-3}\,. \qquad (35)
$$

In comparison, the observed CMB dipole is

$$
D_1^{\rm CMB} = 1.2\times 10^{-3}\,. \qquad (36)
$$

To reconcile this discrepancy, an intrinsic CMB dipole contribution is required:

$$
D_{1,\rm in}^{\rm CMB} \sim 1.4\times 10^{-3}\,. \qquad (37)
$$

Using the relation

$$
D_1 = -(kr_{\rm dec})\cdot 0.27 S_{\rm dec}\,, \qquad (38)
$$

we require

$$
(kr_{\rm dec})S_{\rm dec} \sim \frac{1.5\times 10^{-3}}{0.27} \sim 5\times 10^{-3}\,. \qquad (39)
$$

Thus, an intrinsic dipole of the required magnitude can be obtained without altering the late-time number-count interpretation.

IV. THE EFFECT OF CONTINUOUS SPECTRUM

In realistic models, perturbations are more likely to exhibit a continuous power spectrum than to be dominated by a single mode. For a continuous spectrum, the spherical harmonic coefficients a_{lm} are computed by integrating over all possible wavevectors $\mathbf{k}$. This yields

$$
\begin{aligned}
a_{lm}^{\mathcal{I}} &= 4\pi i^l \int \frac{d^3\mathbf{k}}{(2\pi)^3} X^{\mathcal{I}}(\mathbf{k})\mathcal{T}_l^{\mathcal{I}}(k)Y_{lm}^*(\hat{\mathbf{k}})\,, \\
a_{lm} &= 4\pi i^l \int \frac{d^3\mathbf{k}}{(2\pi)^3}\left(\sum_{\mathcal{I}} X^{\mathcal{I}}(\mathbf{k})\mathcal{T}_l^{\mathcal{I}}(k)\right)Y_{lm}^*(\hat{\mathbf{k}})\,. \qquad (40)
\end{aligned}
$$

The dimensionless power spectrum of X for modes with initial conditions $\mathcal{I}$ and $\mathcal{J}$ is defined as

$$
k^3\left\langle X^{\mathcal{I}}(\mathbf{k})X^{\mathcal{J}}(\mathbf{k}')\right\rangle = (2\pi)^3\delta^{(3)}(\mathbf{k}-\mathbf{k}')\mathcal{P}_{\mathcal{I}\mathcal{J}}(k)\,. \qquad (41)
$$

A straightforward calculation then yields the angular power spectra

$$
\begin{aligned}
C_l^{\mathcal{I}\mathcal{J}} &= \frac{2}{\pi}\int_0^\infty \frac{dk}{k}\mathcal{P}_{\mathcal{I}\mathcal{J}}(k)F_l^{\mathcal{I}}(k)F_l^{\mathcal{J}}(k), \\
C_l &= \frac{2}{\pi}\int_0^\infty \frac{dk}{k}\left(\sum_{\mathcal{I},\mathcal{J}}\mathcal{P}_{\mathcal{I}\mathcal{J}}(k)\right)F_l^{\mathcal{I}}(k)F_l^{\mathcal{J}}(k)\,. \qquad (42)
\end{aligned}
$$

where $\mathcal{T}^{\mathcal{I}}$ and $\mathcal{T}^{\mathcal{J}}$ denote the transfer functions associated with the modes specified by initial conditions $\mathcal{I}$ and $\mathcal{J}$, respectively.

For simplicity, we restrict our attention to the isocurvature mode and define the power spectrum of the superhorizon isocurvature perturbation as

$$k^3 \langle S(\mathbf{k}) S(\mathbf{k}') \rangle = (2\pi)^3 \delta^{(3)}(\mathbf{k}-\mathbf{k}') \mathcal{P}_S(k) \,. \tag{43}$$

In this paper, we consider two types of isocurvature power spectra: a power-law form and another motivated by axion-induced perturbations.

A. Constraints from CMB

The current measurements of the CMB impose stringent constraints on the amplitude of uncorrelated dark matter isocurvature perturbations, which can be quantified as follows [57]:

$$\beta \equiv \left. \frac{\mathcal{P}_S(k)}{\mathcal{P}_R(k)} \right|_{k=k_{\rm pivot}} < 0.038 \,, \tag{44}$$

where $\mathcal{P}_R(k)$ denotes the primordial power spectrum and $k_{\rm pivot}$ is the pivot scale. Planck data impose constraints on the amplitude of dark-matter isocurvature perturbations, requiring the corresponding power spectrum to satisfy $P_S \lesssim 0.8 \times 10^{-10}$ at the wavenumber $k_{\rm pivot} = 0.002\ {\rm Mpc}^{-1}$. This is known as the isocurvature limit and is indicated by the red exclusion region in Fig. 3.

Multipole measurements impose additional constraints on the isocurvature power spectrum. In particular, the quadrupole moment provides the most stringent bounds on superhorizon perturbations, whereas constraints from higher-order multipoles are considerably weaker [33]. Notably, the Planck measurements [48, 49] report a quadrupole value of $\mathcal{D}_2 = 2.26^{+5.33}_{-1.32} \times 10^2\ \mu{\rm K}^2$, while the best-fit ΛCDM model predicts $\mathcal{D}_2 = 1016\ \mu{\rm K}^2$ [48]. Although this discrepancy indicates that the observed quadrupole is lower than the standard-model expectation, these measurements still provide meaningful constraints within the context of our model.

When the quadrupole arises from two different power spectra, their combination must be taken into account. Let $a^{(1)}_{2m}$ and $a^{(2)}_{2m}$ denote the spherical harmonic coefficients corresponding to the two power spectra, $P_1(k)$ and $P_2(k)$, respectively. The combined quadrupole coefficients are given by

$$a_{2m} = a^{(1)}_{2m} + a^{(2)}_{2m} \,. \tag{45}$$

Accordingly, the combined quadrupole power spectrum $\mathcal{D}_2$ is given by

$$\mathcal{D}_2 = \mathcal{D}^{(1)}_2 + \mathcal{D}^{(2)}_2 \,. \tag{46}$$

Given the observed value of $\mathcal{D}^{\rm obs}_2 \simeq 226 \mu{\rm K}^2$, we derive the 2σ upper limit on the quadrupole amplitude as follows:

$$\mathcal{D}_2 \lesssim 1.4 \times 10^3 \mu{\rm K}^2 \,. \tag{47}$$

The quantity $\mathcal{D}_2$, defined here, is related to C_2 in our calculation by

$$\mathcal{D}_2 = \frac{2(2+1)C_2}{2\pi T_0^2} \,, \tag{48}$$

where $T_0 \sim 2.7$ K is the average temperature of the CMB. This upper limit implies an upper bound on the quadrupole component $C^{\rm iso}_2$ generated by the superhorizon isocurvature mode as

$$C^{\rm iso}_2 < 5.5 \times 10^{-11} \,. \tag{49}$$

B. The power-law spectrum

In the first case, $\mathcal{P}_S(k)$ follows a power-law spectrum and is expressed as

$$\mathcal{P}_S(k) = A_I (k/k_{\rm max})^{n-1} \theta(k_{\rm max} - k) \,, \tag{50}$$

where A_I is the amplitude, $k_{\rm max}$ is the maximum comoving wavenumber of isocurvature perturbations, n is the spectral index, which is set to 1 in our calculation, and $\theta(k)$ is the Heaviside step function. Therefore, the angular power spectrum C_l can be written as

$$C_l = \frac{2}{\pi} \int_0^{k_{\rm max}} \frac{dk}{k} \mathcal{P}_S(k) |F_l(k)|^2 \,. \tag{51}$$

C. The axion spectrum

The second power spectrum is given by [33]:

$$\mathcal{P}_S(k) = \mathcal{P}_S(k_{\rm min}) \left[\frac{\varphi(k)}{\varphi(k_{\rm min})} \right]^{-2} \theta(k - k_{\rm min}) \,, \tag{52}$$

where $\mathcal{P}_S(k_{\rm min}) \approx 1$, $k_{\rm min}$ denotes the minimum comoving wavenumber at which the isocurvature perturbation becomes relevant, and $\varphi(k)$ is the radial mode of the axion, governed by

$$\ddot{\varphi} + 3H\dot{\varphi} + V'(\varphi) = 0, \quad V(\varphi) = \frac{\lambda}{4} \left(\varphi^2 - f^2 \right)^2 \,, \tag{53}$$

where f is the axion decay constant and φ is initially displaced slightly from the origin, with a characteristic displacement scale of order H. If this displacement is imprinted on the superhorizon scale set by $k_{\rm min}$, the resulting isocurvature perturbation is enhanced on superhori-

zon scales while remaining small at the scale $k_{\rm dec}$. In this case, the CMB power spectrum can be written as

$$C_l = \frac{2}{\pi}\int_{k_{\rm min}} \frac{dk}{k}\mathcal{P}_S(k)|F_l(k)|^2 \,. \tag{54}$$

In the left panel of Fig. 2, we show the evolution of φ for different values of the parameter λ. In view of the constraints from current CMB observations [48], which imply the bound $H/f \lesssim 10^{-5}$ for $\theta_0 \sim O(1)$, we specify the initial conditions as $\varphi = 0$, $\varphi(k_{\rm min}) = H/\pi$, and $f = 10^5 H$. The right panel shows the corresponding axion isocurvature power spectrum $\mathcal{P}_S(k)$. As the field approaches f, the power spectrum diminishes and eventually becomes negligible. When λ is too small, the power spectrum remains large for too many e-folds, yielding excessive isocurvature perturbations at recombination and violating the isocurvature bound. When λ is too large, the field reaches f too quickly and the superhorizon enhancement becomes too short-lived to generate a sufficiently large dipole.

D. Numerical results

We numerically compute the angular power spectra of the CMB and number-count fluctuations. As in the single-mode case, the number-count dipole and the CMB dipole vanish for adiabatic initial conditions, while the isocurvature CMB dipole does not. To address the dipole tension, Fig. 3 shows the parameter space for both scenarios: the two black curves mark the lower and upper bounds on the dipole amplitude, and the blue regions indicate the 2σ exclusion limits from the observed quadrupole C_2.

The left panel of Fig. 3 shows the parameter space required to explain the cosmic dipole anomaly in the $1/(k_{\rm max}r_{\rm dec})$–$A_I$ plane. In this analysis, the isocurvature constraint is imposed by restricting the parameter space to the region where $k_{\rm max} < k_{\rm dec}$. Within this region, the usual isocurvature bound is automatically satisfied and need not be shown explicitly. We find that explaining the dipole anomaly requires $A_I \gtrsim 0.2$; otherwise, the predicted CMB dipole is too small or the quadrupole becomes too large.

The right panel of Fig. 3 shows the parameter space required to explain the cosmic dipole tension in the $1/(k_{\rm min}r_{\rm dec})$–$\lambda$ plane. The red region is excluded by excessively large isocurvature perturbations. We find that the self-coupling must lie within the range $10^{-9} < \lambda < 4\times10^{-9}$. If future observations determine the axion decay constant f from its couplings, the corresponding scalar mass can also be inferred. For example, if $f \sim 10^{11}$ GeV, the scalar mass is expected to be around $O(10^6)$ GeV. Although this mass is beyond the reach of the current LHC, a future 1000 TeV collider may be capable of detecting this particle.

In axion models, the isocurvature mode does not necessarily vanish abruptly in the power spectrum, and a residual isocurvature component may remain at the recombination scale. Although current observations place only upper limits on the amplitude of isocurvature perturbations, a significant improvement in sensitivity could provide an important cross-check of the axion scenario. In this framework, the axion naturally serves as a dark-matter candidate. For the QCD axion, the mass is typically at the μeV scale. Thus, the existence of the axion particle is a key prediction of this model. Ongoing and future experimental searches for axions will be crucial for testing the viability of the axion scenario.

Before closing this section, we comment on the degree of tuning in our scenario. The allowed regions in Fig. 3 should be viewed as restricted phenomenological windows rather than generic predictions. In the power-law case, explaining the dipole tension requires a sizable

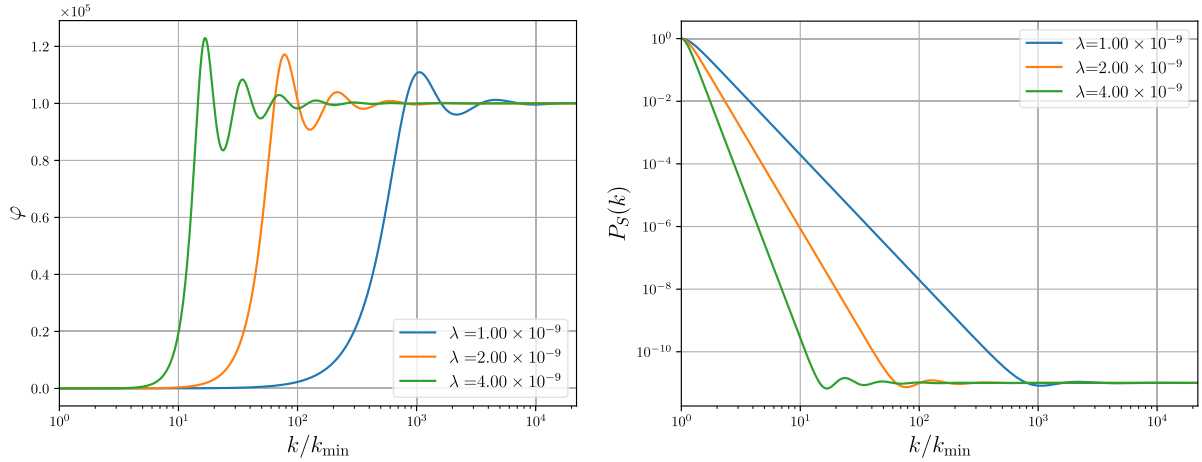

Fig. 2. (color online) [Left] Evolution of the radial mode φ during inflation for $f = 1\times10^5$ and $\lambda = 1\times10^{-9}, 2\times10^{-9}$, and 4×10^{-9}. [Right] Power spectrum $\mathcal{P}_S(k)$ of the isocurvature perturbation induced by the axion for $f = 10^5 H$ and $\lambda = 1\times10^{-9}, 2\times10^{-9}$, and 4×10^{-9}.

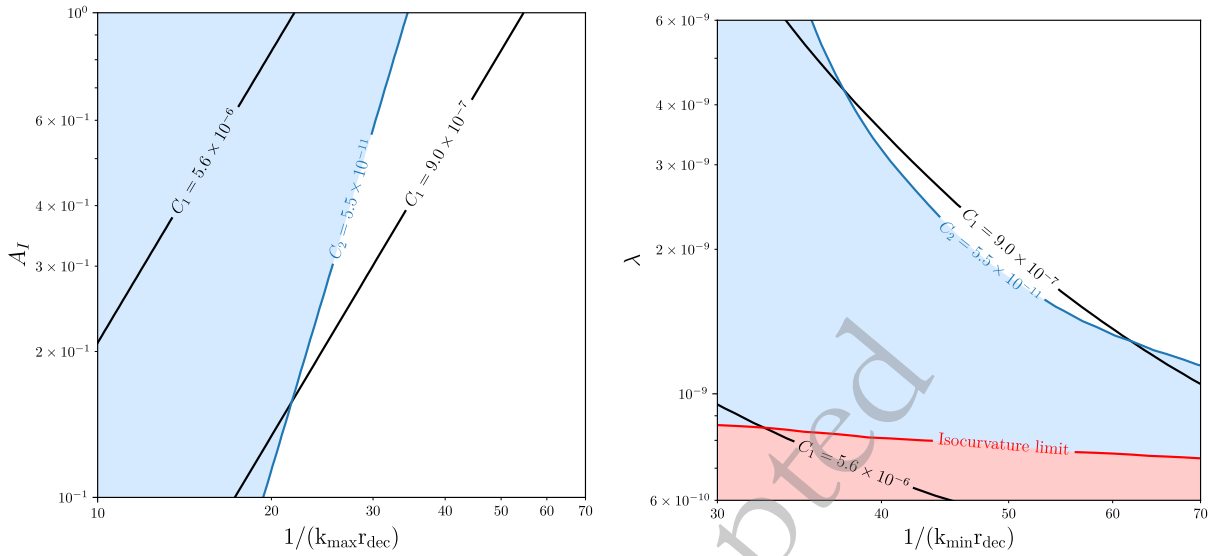

Fig. 3. (color online) Parameter spaces of two models proposed to explain the cosmic dipole problem. The two black curves denote the minimum and maximum amplitudes of the intrinsic CMB dipole required to resolve the tension. The blue regions show the 2σ exclusion limits from the observed quadrupole C_2. The red region is excluded because it would produce excessively large isocurvature perturbations. [Left] Parameter space for the power-law spectrum. [Right] Parameter space for the axion power spectrum.

superhorizon isocurvature amplitude, $A_I \gtrsim 0.2$, together with a cutoff scale sufficiently far beyond the recombination scale such that the usual CMB isocurvature bound is avoided. In the axion case, the viable parameter space results from a balance between two competing effects: if λ is too small, the isocurvature perturbation remains too large at recombination, whereas if λ is too large, the radial field relaxes too quickly and the superhorizon enhancement becomes insufficient. The resulting window, $10^{-9} < \lambda < 4\times10^{-9}$, therefore reflects a certain degree of tuning in the radial-mode dynamics.

This small quartic coupling should be regarded as a property of the radial sector during inflation, rather than as a generic prediction of the QCD axion. Nevertheless, such a small value can be technically stable if the radial mode is sufficiently weakly coupled. For example, if the radial mode couples to the Peccei–Quinn quarks through a Yukawa coupling y, radiative corrections to the quartic coupling are expected to be of order $y^4/(16\pi^2)$. A coupling of order $y \sim 10^{-2}$ gives a correction well below 10^{-9}, and therefore does not destabilize the required value of λ. The main tuning is thus not the radiative stability of a small quartic coupling, but rather the relatively narrow phenomenological interval selected by the dipole and isocurvature constraints. While this window is narrow compared with a generic range of λ, it also makes the scenario predictive and potentially testable.

Since the mechanism mainly modifies the superhorizon isocurvature spectrum, the axion relic abundance can still be determined approximately by the conventional misalignment mechanism. It depends on the axion decay constant, the initial misalignment angle, and the post-inflationary history. A complete model should therefore simultaneously reproduce the observed dark-matter abundance and satisfy the CMB isocurvature bound at recombination.

V. CONCLUSIONS

In this work, we investigate both discrete and continuous power spectra of superhorizon cold dark matter (CDM) isocurvature perturbations as a potential way to resolve the cosmic dipole tension. Our analysis of a single plane-wave perturbation shows that an initial adiabatic superhorizon mode does not contribute to either the CMB dipole or the galaxy number-count dipole. This is because such adiabatic perturbations cancel at leading order. Moreover, the late-time contribution of a superhorizon isocurvature mode to the number-count dipole is strongly suppressed, rendering it ineffective at significantly altering the number-count interpretation. However, a superhorizon isocurvature mode can induce a negative intrinsic dipole in the CMB, partially canceling the kinematic dipole from our peculiar motion and thereby helping to reconcile the observed discrepancy.

We then extend our analysis to continuous spectra of isocurvature fluctuations. Both nearly scale-invariant power-law spectra and axion-generated spectra are capable of resolving the dipole anomaly while remaining consistent with current CMB constraints. For the power-law case, we find that explaining the observed dipole requires $A_I \gtrsim 0.2$ for a suitable cutoff scale k_{max}. In the axion scenario, the evolution of the radial mode during inflation naturally generates large superhorizon iso-

curvature perturbations that decay on recombination scales. We find that, for $f = 10^5 H$ and $10^{-9} < \lambda < 4 \times 10^{-9}$, with an appropriate choice of $k_{\min}$, the observed dipole tension can be resolved.

If confirmed, this mechanism would not only address the cosmic dipole problem but also provide indirect support for the existence of axion dark matter. However, the axion interpretation remains model-dependent, especially regarding the origin of the small quartic coupling and its relation to the final dark matter abundance. Our results thus preserve the cosmological principle while motivating further investigation into the generation of superhorizon fluctuations and the broader implications of axion physics in the early Universe.

ACKNOWLEDGMENTS

C. H. acknowledges support from the Sun Yat-sen University Science Foundation, the Fundamental Research Funds for the Central Universities at Sun Yat-sen University under Grant No. 24qnpy117, and the Key Laboratory of Particle Astrophysics and Cosmology (MOE) at Shanghai Jiao Tong University.

References

[1] G. F. R. Ellis and J. E. Baldwin, Monthly Notices of the Royal Astronomical Society **206**, 377 (1984)
[2] J. J. Condon, W. D. Cotton, E. W. Greisen, Q. F. Yin, R. A. Perley, G. B. Taylor, *et al*, The Astronomical Journal **115**, 1693 (1998)
[3] R. Maartens, C. Clarkson and S. Chen, Journal of Cosmology and Astroparticle Physics **2018**, 013 (2018)
[4] T. Nadolny, R. Durrer, M. Kunz and H. Padmanabhan, Journal of Cosmology and Astroparticle Physics **2021**, 009 (2021)
[5] C. Gibelyou and D. Huterer, Monthly Notices of the Royal Astronomical Society **427**, 1994 (2012)
[6] T. Mauch, T. Murphy, H. J. Buttery, J. Curran, R. W. Hunstead, B. Piestrzynski, *et al*, Monthly Notices of the Royal Astronomical Society **342**, 1117 (2003)
[7] Y. Itoh, K. Yahata and M. Takada, Physical Review D **82**, 043530 (2010)
[8] A. K. Singal, The Astrophysical Journal **742**, L23 (2011)
[9] M. Rubart and D. J. Schwarz, Astronomy & Astrophysics **555**, A117 (2013)
[10] P. Tiwari and A. Nusser, Journal of Cosmology and Astroparticle Physics **2016**, 062 (2016)
[11] A. K. Singal, Physical Review D **100**, 063501 (2019)
[12] T. M. Siewert, M. Schmidt-Rubart and D. J. Schwarz, Astronomy & Astrophysics **653**, A9 (2021)
[13] N. Secrest, S. v. Hausegger, M. Rameez, R. Mohayaee, S. Sarkar and J. Colin, The Astrophysical Journal Letters **908**, L51 (2021)
[14] N. Secrest, S. v. Hausegger, M. Rameez, R. Mohayaee and S. Sarkar, The Astrophysical Journal Letters **937**, L31 (2022)
[15] N. Secrest, S. von Hausegger, M. Rameez, R. Mohayaee and S. Sarkar, Reviews of Modern Physics **97**, 041001 (2025)
[16] P. K. Aluri, P. Cea, P. Chingangbam, M.-C. Chu, R. G. Clowes, D. Hutsemékers, *et al*, Classical and Quantum Gravity **40**, 094001 (2023)
[17] L. Dam, G. F. Lewis and B. J. Brewer, Mon. Not. Roy. Astron. Soc. **525**, 231 (2023), arXiv: 2212.07733
[18] O. T. Oayda, V. Mittal, G. F. Lewis and T. Murphy, Mon. Not. Roy. Astron. Soc. **531**, 4545 (2024), arXiv: 2406.01871
[19] J. Darling, The Astrophysical Journal Letters **931**, L14 (2022)
[20] A. Abghari, E. F. Bunn, L. T. Hergt, B. Li, D. Scott, R. M. Sullivan, *et al*, Journal of Cosmology and Astroparticle Physics **2024**, 067 (2024)
[21] S. Mittal, G. Kulkarni, D. Anstey and E. d. L. Acedo, Monthly Notices of the Royal Astronomical Society **534**, 1317 (2024)
[22] A. L. Erickcek, C. M. Hirata and M. Kamionkowski, Physical Review D **80**, 083507 (2009)
[23] G. Domènech, R. Mohayaee, S. P. Patil and S. Sarkar, Journal of Cosmology and Astroparticle Physics **2022**, 019 (2022)
[24] M. S. Turner, General Relativity and Gravitation **24**, 1 (1992)
[25] A. L. Erickcek, S. M. Carroll and M. Kamionkowski, Physical Review D **78**, 083012 (2008)
[26] K. Tomita, The Astrophysical Journal **529**, 26 (2000)
[27] Y.-Z. Ma, C. Gordon and H. A. Feldman, Physical Review D **83**, 103002 (2011)
[28] J. Colin, R. Mohayaee, M. Rameez and S. Sarkar, Astronomy & Astrophysics **631**, L13 (2019)
[29] C. T. Byrnes and E. R. M. Tarrant, Journal of Cosmology and Astroparticle Physics **2015**, 007 (2015)
[30] C. Byrnes, G. Domènech, M. Sasaki and T. Takahashi, Journal of Cosmology and Astroparticle Physics **2016**, 020 (2016)
[31] Q. Yang, Y. Liu and H. Di, Physical Review D **96**, 083516 (2017)
[32] E. Ebrahimian, C. Krishnan, R. Mondol and M. M. Sheikh-Jabbari, Class. Quant. Grav. **41**, 145007 (2024), arXiv: 2305.16177
[33] C. Han, Physical Review D **108**, 015026 (2023)
[34] R. D. Peccei and H. R. Quinn, Physical Review Letters **38**, 1440 (1977)
[35] R. D. Peccei and H. R. Quinn, Phys. Rev. D **16**, 1791 (1977)
[36] P. J. Steinhardt and M. S. Turner, Physics Letters B **129**, 51 (1983)
[37] J. Preskill, M. B. Wise and F. Wilczek, Physics Letters B **120**, 127 (1983)
[38] M. Dine and W. Fischler, Physics Letters B **120**, 137 (1983)
[39] L. F. Abbott and P. Sikivie, Physics Letters B **120**, 133 (1983)
[40] D. Seckel and M. S. Turner, Physical Review D **32**, 3178 (1985)
[41] D. H. Lyth, Physics Letters B **236**, 408 (1990)
[42] M. S. Turner and F. Wilczek, Physical Review Letters **66**, 5

(1991)
[43] A. Linde, Physics Letters B **259**, 38 (1991)
[44] J. E. Kim and G. Carosi, Rev. Mod. Phys. **82**, 557 (2010), arXiv: 0807.3125
[45] O. Wantz and E. P. S. Shellard, Physical Review D **82**, 123508 (2010)
[46] D. J. E. Marsh, Physics Reports **643**, 1 (2016)
[47] X. Chen, J. Fan and L. Li, *New inflationary probes of axion dark matter*, Feb., 2024. 10.48550/arXiv.2303.03406.
[48] Planck Collaboration, Astronomy & Astrophysics **641**, A6 (2020)
[49] Planck Collaboration, Astronomy & Astrophysics **641**, A1 (2020)
[50] C. Dalang and C. Bonvin, Monthly Notices of the Royal Astronomical Society **512**, 3895 (2022)
[51] R. Durrer, *The Cosmic Microwave Background*. Cambridge University Press, 2 ed., 2020.
[52] C. Bonvin and R. Durrer, Physical Review D **84**, 063505 (2011)
[53] A. Challinor and A. Lewis, Physical Review D **84**, 043516 (2011)
[54] J. P. Zibin and D. Scott, Physical Review D **78**, 123529 (2008)
[55] D. Blas, J. Lesgourgues and T. Tram, Journal of Cosmology and Astroparticle Physics **2011**, 034 (2011)
[56] E. Di Dio, F. Montanari, J. Lesgourgues and R. Durrer, Journal of Cosmology and Astroparticle Physics **2013**, 044 (2013)
[57] Planck Collaboration, Astronomy & Astrophysics **641**, A10 (2020)